

Scientific paper

Electroreduction of Some Substituted Hydrazones on Platinum Electrode in Dimethylformamide

Ayça Demirel Özel,^{1,*} Zehra Durmuş,¹ İbrahim Yılmaz,²
Alaaddin Çukurovalı³ and Esmâ Kılıç¹

¹ Department of Chemistry, Faculty of Science, Ankara University, Ankara, Turkey

Faculty of Science, Karamanoğlu Mehmetbey University, Karaman

³ Department of Chemistry, Faculty of Arts and Sciences, Firat University, Elazığ, Turkey

* Corresponding author: E-mail: aycaozel@gmail.com;
Tel.: +90 312 2126720/1269; Fax: +90 312 2232395

Received: 18-12-2008

Abstract

The electrochemical behaviors of 4-(1-phenyl-1-methylcyclobutane-3-yl)-2-(2-hydroxybenzylidenehydrazino)thiazole (I), 4-(1-*p*-xylene-1-methylcyclobutane-3-yl)-2-(2-hydroxybenzylidenehydrazino)thiazole (II), 4-(1-mesitylene-1-methylcyclobutane-3-yl)-2-(2-hydroxybenzylidenehydrazino)thiazole (III), 4-(1-phenyl-1-methylcyclobutane-3-yl)-2-(2-hydroxy-5-bromobenzylidenehydrazino)thiazole (IV), 4-(1-phenyl-1-methylcyclobutane-3-yl)-2-(2-hydroxy-3-methoxybenzylidenehydrazino)thiazole (V), 4-(1-phenyl-1-methylcyclobutane-3-yl)-2-(2,4-dihydroxybenzylidenehydrazino)thiazole (VI) were investigated by cyclic voltammetry (CV), controlled potential electrolysis, and chronoamperometry (CA) techniques in the presence of 0.10 M tetrabutylammonium tetrafluoroborate (TBATFB) in dimethylformamide (DMF) at platinum electrode. Hydrazones display two cathodic peaks at about –1.60 V and –2.20 V. Diffusion coefficients and the number of electrons transferred were calculated by using an ultramicro electrode (UME). Standard heterogeneous rate constants for reduction were calculated by Klinger-Kochi technique. Electrochemical reduction mechanism of these hydrazones was also proposed that hydrazones seemed to follow an ECEC mechanism corresponding with irreversible electron transfer steps. Due to the widespread use of hydrazones in drug production, the redox properties of these hydrazones are thought to be useful for enlightening the metabolic fate of the drug containing hydrazones or its *in vivo* redox properties or pharmacological activity.

Keywords: Hydrazones, thiazoles, electrochemical behavior, voltammetry, dimethylformamide

1. Introduction

One important class of heterocyclic compounds which contains one sulfur atom is known as thiazole. This class of compounds is present in many natural and synthetic products with a wide range of pharmacological activities such as antiviral, anticancer, antibacterial, antifungal, anti-parkinsonian activities that can be well illustrated by the large number of drugs in market containing this functional group.¹ Thiazole ring also finds applications in other fields such as polymers,² liquid crystals,³ photonucleases,⁴ fluorescent dyes,⁵ insecticides⁶ and antioxidants.⁷

Thiazoles include different compounds such as hydrazones. In this study, hydrazones containing both

thiazole ring and cyclobutane group were investigated. It is a well-known fact that the hydrazone group plays an important role in the anti-microbial activity.^{8–10} 3-substituted cyclobutane carboxylic acid derivatives exhibit anti-inflammatory and anti-depressant activities^{11,12} and liquid crystal properties.¹³ In addition, many of the physiologically active hydrazones find applications in the treatment of diseases like tuberculosis, leprosy and mental disorder.¹⁴ Cyclobutane derivatives are also used in some drugs for above mentioned diseases. For this reason, knowledge of the electrochemical behaviour of the hydrazones may be very helpful for their efficient uses. Elucidation of electrochemical mechanism of the reduction and the oxidation at the electrode surface can be useful to suggest mechanisms for the biochemical behaviour of hydrazones, in ot-

her words electroreduction mechanism can serve as models for the biological pathway¹⁵ because, their activity in the body depends on reductive processes. The chemical and biological activity of these compounds would vary in different media. A good knowledge of the electrochemical behaviour of hydrazones in dimethylformamide (DMF) is, therefore, of considerable interest. Accordingly, the knowledge of the electrochemical reduction of these hydrazones is a prerequisite to understand their mechanism in both chemical and biological processes.^{16,17} Also, electrochemical methods can be used to generate intermediates. The reduction of several hydrazones has been investigated successfully by electrochemical techniques.

The first systematic study on the electrochemical reduction of hydrazones was published by Lund several decades ago.¹⁸ Since then, electrochemical behavior of hydrazones has been investigated in both protic^{19–40} and aprotic solvents.^{39–56} Under aqueous conditions, the reduction consists of two-electron, two-proton transfer, which converts the C=N–NH to CH–NH–NH group.^{18,23,28} In aprotic solvents, where hydrolysis of the iminic moiety is hampered, various studies of the electroreduction of imines have appeared in the literature.^{39–56} Electrochemical reduction of various imines was studied by Andrieux et al. in acetonitrile and DMF medium.⁴⁶ They claimed that, according to the structure of the imine and the solvent, the reduction was either a two-electron transfer or two one-electron transfers. Isse et al. investigated the electrochemical reduction of the Schiff bases in DMF. The reduction process involves self-protonation reactions. The two-electron reduction product is formed together with the conjugate base of the Schiff bases.⁴⁴ Kononenko et al. claimed that the first wave observed in the electrochemical reduction of imine group of Schiff bases in DMF was an irreversible two-electron transfer reaction and overall process is controlled by diffusion of the depolarizer to the electrode.⁵⁷ Fry and Reed investigated the electrochemical reduc-

tion of several imines in DMF containing tetraethylammonium bromide using cyclic voltammetry, coulometry and polarography.⁴⁵ They indicated that an irreversible two-electron reduction occurred and that a radical anion formed in the first step followed rapid proton abstraction and a second electron transfer.

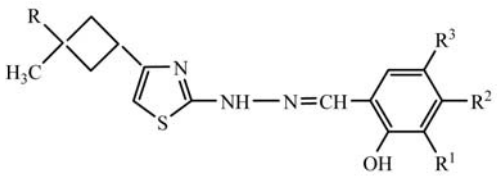
Therefore, it is essential to elucidate the electrochemical reduction of hydrazones containing cyclobutane, 2-aminothiazole and Schiff base characteristic. The investigated hydrazones have not been studied at platinum electrode and polarographically at mercury electrode so far. In this study, the electrochemical behavior of some substituted hydrazones in DMF at platinum electrode was investigated using electrochemical techniques. The hydrazones are given in Table 1. The diffusion coefficient, the number of electrons transferred, standard heterogeneous rate constants (k_s), adsorption properties and the reduction mechanisms of these hydrazones were investigated using cyclic voltammetry, chronoamperometry and IR spectroscopy.

2. Experimental

2.1. Reagents

Hydrazones were prepared as described in the literature.^{58–63} The hydrazones were purified by recrystallization from ethanol until a sharp melting point was obtained (Table 2). The structures of these hydrazones were elucidated by using IR, ¹H–NMR and magnetic susceptibility.^{58–63} No impurities on thin layer chromatography (TLC) plates and ¹H–NMR spectra were observed. All chemicals were of analytical reagent grade (Merck and Sigma). Stock solutions of each hydrazone were prepared at a concentration of 5.0×10^{-3} M in 0.1 M TBATFB/DMF. Voltammetric working solutions were prepared by diluting the stock solutions to obtain the desired concentrations. The supporting electrolyte of tetrabutylammo-

Table 1. The Chemical Structures and the Names of the Hydrazones Investigated

					
General formula		R	R ¹	R ²	R ³
Hydrazone	Names				
I	4-(1-phenyl-1-methylcyclobutane-3-yl)-2-(2-hydroxybenzylidenehydrazino)thiazole	benzene	H	H	H
II	4-(1- <i>p</i> -xylene-1-methylcyclobutane-3-yl)-2-(2-hydroxybenzylidenehydrazino)thiazole	<i>p</i> -xylene	H	H	H
III	4-(1-mesitylene-1-methylcyclobutane-3-yl)-2-(2-hydroxybenzylidenehydrazino)thiazole	mesitylene	H	H	H
IV	4-(1-phenyl-1-methylcyclobutane-3-yl)-2-(2-hydroxy-5-bromobenzylidenehydrazino)thiazole	benzene	H	H	Br
V	4-(1-phenyl-1-methylcyclobutane-3-yl)-2-(2-hydroxy-3-methoxybenzylidenehydrazino)thiazole	benzene	OCH ₃	H	H
VI	4-(1-phenyl-1-methylcyclobutane-3-yl)-2-(2,4-dihydroxybenzylidenehydrazino)thiazole	benzene	H	OH	H

nium tetrafluoroborate (TBATFB) was purchased from Fluka (21796-4) and used without further purification. The DMF used was a dry (water ≤ 0.01 %) batch of Fluka (40248) kept on beads of a molecular sieve.

Table 2. Melting Points and Elemental Analysis Results of Hydrazones.

	I	II	III	IV	V	VI
Melting Points ($^{\circ}\text{C}$)	194	168	225	201	159	173
Elemental Analysis Results, Calculated (Found), %	C 69.39 (69.79) H 5.82 (4.82) N 11.56 (11.25) S 8.82 (9.12)	C 70.56 (71.14) H 6.44 (5.89) N 10.73 (10.84) S 8.19 (8.29)	C 71.19 (71.08) H 6.71 (6.60) N 10.36 (10.40) S 7.91 (7.72)	C 57.02 (56.69) H 4.56 (4.41) N 9.50 (9.67) S 7.25 (7.44)	C 67.15 (67.03) H 5.89 (6.10) N 10.68 (10.54) S 11.07 (10.87)	C 66.47 (66.03) H 5.58 (5.64) N 8.15 (8.22) S 8.45 (8.18)

2. 2. Apparatus

Voltammetric measurements were carried out with BAS100 B/W Electrochemical Analyzer. Platinum electrode (BAS MF-2013, 1.6 mm diameter) and 100 μm -ultramicro platinum electrode (BAS MF-2150) were used as a working electrode. The electrodes were polished before each use with 1 μm , 0.3 μm and 0.05 μm alumina slurries made from dry Buehler alumina and ultra pure water (18 M Ωcm) on polishing microcloth. Polished Pt electrode was then sonicated in a mixture of 50:50 (v/v) methanol/DMF. A platinum wire was used as the auxiliary electrode (BAS MW-1032). The reference electrode was a silver wire in contact with 0.01 M AgNO_3 in dimethylformamide. All solutions were deaerated for 10 min. with pure argon. All the measurements were taken at room temperature, 21 ± 1 $^{\circ}\text{C}$. In all voltammetric measurements, the background currents were automatically subtracted from originally obtained currents. IR spectra were obtained from Mattson 1000 FTIR Spectrometer.

2. 3. Method

The number of electrons transferred and diffusion coefficients were determined by ultramicro electrode CV technique of Baranski.⁶⁴ Also, the data obtained from bulk electrolysis were used to calculate the number of electrons transferred. For this purpose, coulometric studies were carried out on a BAS 100 B/W instrument with a working electrode of reticulated vitreous carbon electrode (MF-2077) in DMF containing 0.1 M TBATFB. A three-electrode circuit was used including the Ag/Ag^+ electrode as a reference and coiled platinum wire (23 cm) (MW-1033) as a counter electrode. The solution was mixed with a magnetic stirrer. The applied potentials were 50 mV more negative than each peak potential. The heterogeneous rate

constants were calculated according to Klingler-Kochi method.⁶⁵

3. Results and Discussion

3. 1. Characterization of the Electrode Reaction

Fig. 1 displays the cyclic voltammograms of 5.0×10^{-3} M hydrazone derivatives listed in Table 1 in 0.1 M TBATFB/ DMF system at a scan rate of 0.1 V/s together with the voltammogram of the blank solution. The cyclic voltammograms of the hydrazones revealed two cathodic and two anodic peaks as shown in Fig. 1. The peak potentials are listed in Table 3. The voltammetric reduction of hydrazones in DMF containing 0.1 M TBATFB gives rise to two cathodic peaks. There are no redox peak couples. But, the voltammograms, reversed after the first(A) and second(B) peaks, showed that the first and second cathodic peaks are related to first(D) and second(C) anodic peaks, respectively.

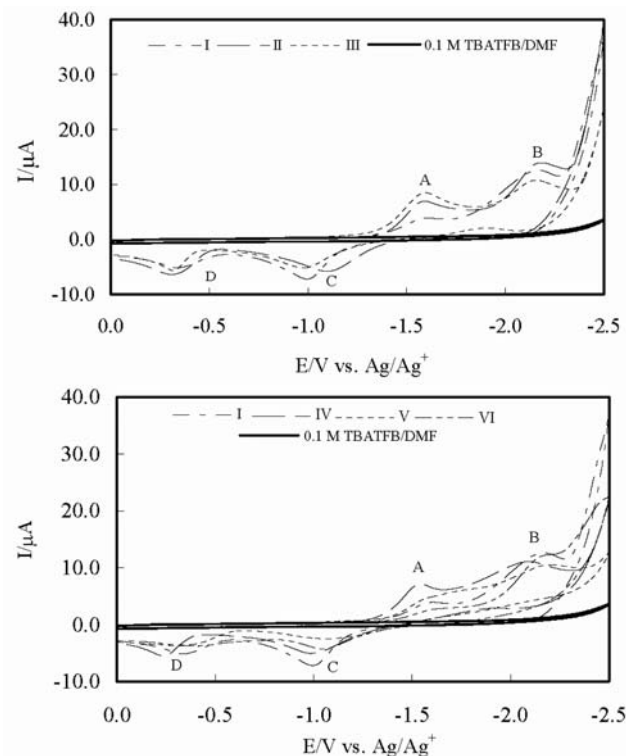
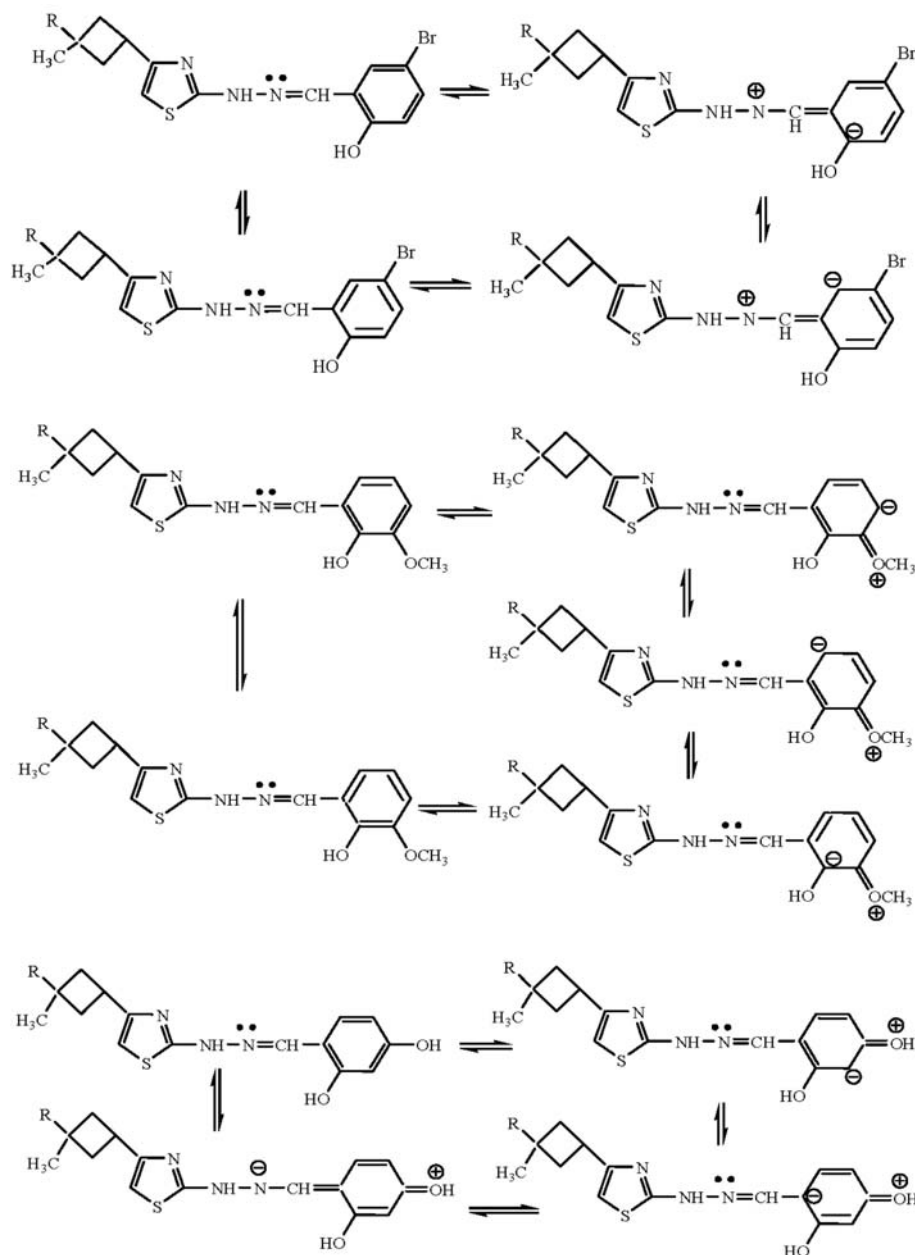


Fig. 1. Cyclic voltammograms of I, II, III, IV, V, and VI in DMF containing 0.1 M TBATFB on Pt electrode at a scan rate of 0.10 Vs^{-1} (vs. Ag/Ag^+).

The data obtained from Fig. 1 and listed in Table 3 were used to investigate the relation between the reduction potentials and the substituent effect. It was observed that the cathodic and anodic peak potentials of hydrazo-

Table 3. Cyclic Voltammetric Data for the Reduction of Hydrazones I to VI

Hydrazone I					Hydrazone II					Hydrazone III				
ν , V/s	E_{pA}^c/V	E_{pD}^a/V	E_{pB}^c/V	E_{pC}^a/V	ν , V/s	E_{pA}^c/V	E_{pD}^a/V	E_{pB}^c/V	E_{pC}^a/V	ν , V/s	E_{pA}^c/V	E_{pD}^a/V	E_{pB}^c/V	E_{pC}^a/V
0.1	-1.59	-0.33	-2.17	-1.00	0.1	-1.59	-0.31	-2.17	-1.11	0.1	-1.59	-0.32	-2.16	-1.00
0.5	-1.64	-0.29	-2.26	-0.92	0.5	-1.64	-0.28	-2.34	-1.01	0.5	-1.71	-0.29	-2.26	-0.89
1.0	-1.68	-0.28	-2.37	-0.89	1.0	-1.67	-0.26	-2.45	-0.89	1.0	-1.73	-0.27	-2.35	-0.85
Hydrazone IV					Hydrazone V					Hydrazone VI				
ν , V/s	E_{pA}^c/V	E_{pD}^a/V	E_{pB}^c/V	E_{pC}^a/V	ν , V/s	E_{pA}^c/V	E_{pD}^a/V	E_{pB}^c/V	E_{pC}^a/V	ν , V/s	E_{pA}^c/V	E_{pD}^a/V	E_{pB}^c/V	E_{pC}^a/V
0.1	-1.53	-0.25	-2.04	-1.03	0.1	-1.58	-0.31	-2.15	-1.07	0.1	-1.64	-0.43	-2.18	-1.11
0.5	-1.69	-0.20	-2.20	-0.93	0.5	-1.71	-0.25	-2.35	-0.89	0.5	-1.66	-0.39	-2.25	-0.99
1.0	-1.72	-0.18	-2.25	-0.89	1.0	-1.73	-0.24	-2.39	-0.87	1.0	-1.68	-0.37	-2.28	-0.92

Fig. 2. Resonance and inductive effects of the substituents on the $-\text{CH}=\text{N}-\text{NH}-$ group of hydrazone derivatives.

nes **I**, **II** and **III** where the substituent group R are benzene, *p*-xylene and mesitylene were very close almost identical to each other. This may be attributed to the fact that these groups are located to very far from the group (–CH=N–NH–) where the electroreduction takes place.

However, the reduction potentials of hydrazone derivatives **I**, **IV**, **V** and **VI**, where R group is benzene but R¹, R² and R³ groups are positioned differently were observed to differ from each other. As can be seen from Table 3, these three groups are –H in hydrazone **I** but R³ = Br in **IV**; R¹ = OCH₃ in **V** and R² = OH in **VI**. The inductive and resonance effects of these substituents will obviously have a large effect on the electron density of –CH=N–NH– group. The electronic effects of these substituents on –CH=N–NH– group are shown in Fig. 2.

When we consider hydrazone **I** where R¹, R² and R³ are –H and R is benzene and hydrazone **IV** where R³ is –Br, it is seen that the insertion of Br into the structure causes in decreased electron density on –CH=N–NH– group and facilitates the reduction process through the inductive effect which explains the fact that the reduction potential of **IV** is more positive than the reduction potential of **I** (Fig. 1 and Table 3).

Similarly, when the reduction potentials of **I** and **V** (where R¹ is –OCH₃) are examined, it is seen that the replacement of –H with –OCH₃ does not have a significant effect on the electron density of –CH=N–NH– group. That is why the reduction potentials of hydrazones **I** and **V** are almost the same (Fig. 1 and Table 3).

When the reduction potentials of **I** and **VI** (where R² is –OH) is compared, it is observed that the insertion of hydroxyl group at the para position, increases the electron density on –CH=N–NH– group and makes the reduction process more difficult which is manifested by a negative shift in reduction potential (Fig. 1 and Table 3).

The cyclic voltammograms in Fig. 1 suggest that the reduction processes of six hydrazone derivatives investigated are similar. These voltammograms can also be used to decide the reversibility of the reactions. When the voltammograms were reversed after each peak, it was observed that the peak(D) appeared after the first peak(A) and peak(C) was observed after the second peak(B) (Fig. 1). As can be seen from the voltammograms, the difference between the cathodic and anodic peak potentials is rather large (> 1.00 V). This is highly typical for the quasi-reversible reaction complicated by a chemical reaction. It is also observed from Table 3 that the peak potentials show a negative shift as the scan rate is increased.

The fact that E_p^c values show a negative shift at higher scan rates is a clear indication of an irreversible behaviour.^{66,67} This was also verified by the decrease of the current function ($i_p^c/v^{1/2}$) with increasing scan rate (v) graphs. This is a further proof that a chemical step takes place after the electron transfer process.

The simplest way to understand whether the hydrazone derivatives investigated make a strong adsorption on

to the electrode surface is the appearance of another peak at more positive or negative potentials than the reduction peak. There were no such pre- or post- peaks observed for any of the hydrazones investigated which indicated the absence of strong adsorption. Also, the fact that the slopes of $\log(i_p^c/\mu A)$ vs. $\log(v/V/s)$ were less than 0.5 for both the first and the second peak was further verification of this situation.⁶⁸ Therefore, it can conveniently be claimed that the reactions investigated are not controlled by adsorption phenomenon. The linearity of i_p^c vs. $v^{1/2}$ graphs indicates that the reactions are diffusion controlled.⁶⁷

3. 2. Determination of the Number of Electrons Transferred and the Diffusion Coefficients

The number of electrons transferred during the reduction of hydrazone **I** to **VI** and the diffusion coefficients were calculated by both cyclic voltammetry at ultramicro electrode and Chronoamperometry.⁶⁴ n and D values were calculated according to the equations below.

$$D = \frac{D_s S_s^2 i^2}{S^2 i_s^2} \quad (1)$$

$$n = \frac{n_s S_s^2 i_s C_s}{S_s^2 i C} \quad (2)$$

Here, i is limiting steady-state current, C is the concentration, S is the slope of the chronoamperometric i vs $t^{-1/2}$ plot for hydrazones. n_s , D_s and C_s are the same values obtained for ferrocene-ferrocenium reference redox couple. The experimental values of n and D for all hydrazones are given in Table 4. In order to determine the limiting steady-state currents for hydrazones, linear sweep voltammetry was also used. The number of electrons transferred during the reduction of hydrazone **I** to **VI** was also determined by bulk electrolysis.

The number of electrons transferred calculated with the use of UME was in good accordance with the number of electrons determined from bulk electrolysis (Table 4). The diffusion coefficients obtained are given in Table 4. The fact that the diffusion coefficients of all the hydrazones are similar proves the fact that they diffuse to the electrode surface in a similar manner due to their closely related structures.

3. 3. Klingler-Kochi Method for Determination of the Heterogeneous Electron-Transfer Standard Rate Constants

The heterogeneous electron-transfer standard rate constants are found from cyclic voltammogram data in the different scan rates. In general, as the scan rate is increa-

Table 4. Diffusion Coefficients, Number of Electrons, Heterogeneous Standard Rate Constants for Hydrazones I to VI in Dimethylformamide at Pt Electrode^a

Hydrazone	The number of electrons transferred per molecule determined at ultramicro Pt electrode by UME-CV technique of Baranski, <i>n</i>		Number of electrons calculated at reticulated vitreous carbon electrode by Bulk Electrolysis, <i>n</i>		Total number of electrons calculated by Bulk Electrolysis, <i>n_T</i>	Diffusion coefficients (<i>D</i>), cm ² /s <i>D</i> ± <i>ts</i> /√ <i>N</i>	Standard rate constants, (<i>k_s</i>), cm/s <i>k_s</i> ± <i>ts</i> /√ <i>N</i>
	Peak A	Peak B	Peak A	Peak B			
I	2.01 ± 0.07	0.93 ± 0.01	1.98 ± 0.03	1.00 ± 0.30	3.13 ± 0.17	3.28 × 10 ⁻⁶ ± 0.02 × 10 ⁻⁶	1.35 × 10 ⁻⁵ ± 0.65 × 10 ⁻⁵
II	–	1.29 ± 0.06	1.92 ± 0.10	1.10 ± 0.22	2.63 ± 0.11	3.22 × 10 ⁻⁶ ± 0.76 × 10 ⁻⁶	1.18 × 10 ⁻⁵ ± 0.14 × 10 ⁻⁵
III	2.04 ± 0.10	0.75 ± 0.17	2.06 ± 0.01	0.87 ± 0.03	3.10 ± 0.10	3.07 × 10 ⁻⁶ ± 0.65 × 10 ⁻⁶	9.66 × 10 ⁻⁶ ± 0.18 × 10 ⁻⁶
IV	1.82 ± 0.04	0.95 ± 0.11	–	–	2.67 ± 0.24	2.47 × 10 ⁻⁶ ± 0.23 × 10 ⁻⁶	3.64 × 10 ⁻⁶ ± 0.20 × 10 ⁻⁶
V	–	0.46 ± 0.01	1.91 ± 0.20	–	2.71 ± 0.13	3.19 × 10 ⁻⁶ ± 0.15 × 10 ⁻⁶	3.10 × 10 ⁻⁶ ± 0.23 × 10 ⁻⁶
VI	1.68 ± 0.20	–	–	–	3.09 ± 0.30	3.23 × 10 ⁻⁶ ± 0.30 × 10 ⁻⁶	2.38 × 10 ⁻⁶ ± 0.13 × 10 ⁻⁶

^a at 95% confidence level; t: 3.18; s: standard deviation; N = 4

sed, E_p^c and the peak width values ($E_{p/2}$), show a change which affects the value of k_s . The results, obtained from the formulas below, showed that the k_s vs $v^{1/2}$ plot had a plateau at high scan rates. In our case, this plateau starts as the scan rate exceeds $\sim 2.0 \text{ Vs}^{-1}$. The average k_s values in this plateau at 21 °C, which are independent of v , are tabulated in Table 4. The fact that these k_s values are $k_s < 2 \times 10^{-5} v^{1/2}$ is another indication of irreversible behavior.⁶⁵

$$k_s = 2.18 \left(\frac{D\beta n F v}{RT} \right)^{1/2} \quad \beta = 1.857 \frac{RT}{nF(E_p^c - E_{p/2}^c)}$$

3. 4. Mechanistic Studies

In Table 6, the number of total electrons transferred was found as 3 for all the hydrazones investigated. It was determined that there were 2 electron transfer in the first and a one electron transfer in the second peak. Thus, it was concluded that all the hydrazones follow the same reduction mechanism.

The first reduced center in these hydrazones is the $-\text{N}=\text{CH}-$ double bond which accepts two electrons to form the corresponding dianion (**b**). The $2e^-$ reduction of $-\text{CH}=\text{N}-\text{NH}-$ group which occur at peak(A) was thought to take place as depicted in Step 1 (Fig. 3). The formed dianion (**b**) would be strong base enough to abstract protons from parent molecule (**a**) and a chemical reaction would occur (Step 2).

In 1964, Nicholson and Shain solved some complex differential equations by using Fick's First Law, Nernst Equation, Randles-Sevcik Equation and found out the relation between the peak current, scan rate and the chemical reactions.⁶⁶ Several expressions including different parameters such as $i_p^c/v^{1/2}C$ were applied to electrode reactions and it was found that successive chemical reactions had affected the shape of the voltammograms and the reaction rate. One of these parameters is the graph of cur-

rent function ($i_p^c/v^{1/2}C$) values against scan rate (v). Here, $i_p^c / \mu\text{A}$ is the cathodic peak current; $v^{1/2}$ is the square root of scan rate and C/M is the concentration of hydrazones. As it is obvious in the figure below, if an exponential decrease is met towards increasing scan rates, this indicates that the electron transfer is followed by a chemical reaction (Fig. 4).

For the first cathodic peak, the current function ($i_p^c/v^{1/2}C$) values were plotted against the scan rate (v) in order to apply the Nicholson-Shain criteria,⁶⁶ to elucidate the reaction mechanism taking place at the first peak and the plot obtained is given in Fig. 4. As shown in figure, the fact that the current function decrease exponentially towards the higher scan rates is an indication that the electron transfer is followed by a chemical reaction as shown in Step 2 and the corresponding mechanism to the peak(A) was suggested EC type (Step 1, Step 2). In absence of chemical complications, this graph would be expected to be a nearly horizontal line.⁶⁶

To ensure that a conjugate base is formed as a result of a homogeneous chemical reaction, voltammetric experiments were also performed with the addition of acetic acid. There were various concentrations of acetic acid added to 0.1 M TBATFB/ DMF solutions of the hydrazones to see whether any changes in the resulting voltammograms occur (Fig. 5). As seen from the figure, the addition of certain amount of acetic acid to 5.0×10^{-3} M solution of hydrazone I resulted an increase in peak(A) and a decrease in peak(B). This suggested us that the second reduction peak belongs to the reduction of the conjugate base of hydrazone.^{42, 44} This behaviour provides a first indication that the second peak is attributable to the reduction of the conjugate base (**d**), which is the conjugate base form of parent molecule in solution as indicated in Fig. 6. The chemical reaction occurring after first reduction (Step 2) was thought to be a proton transfer step from OH groups in the non reduced molecules in the solution.

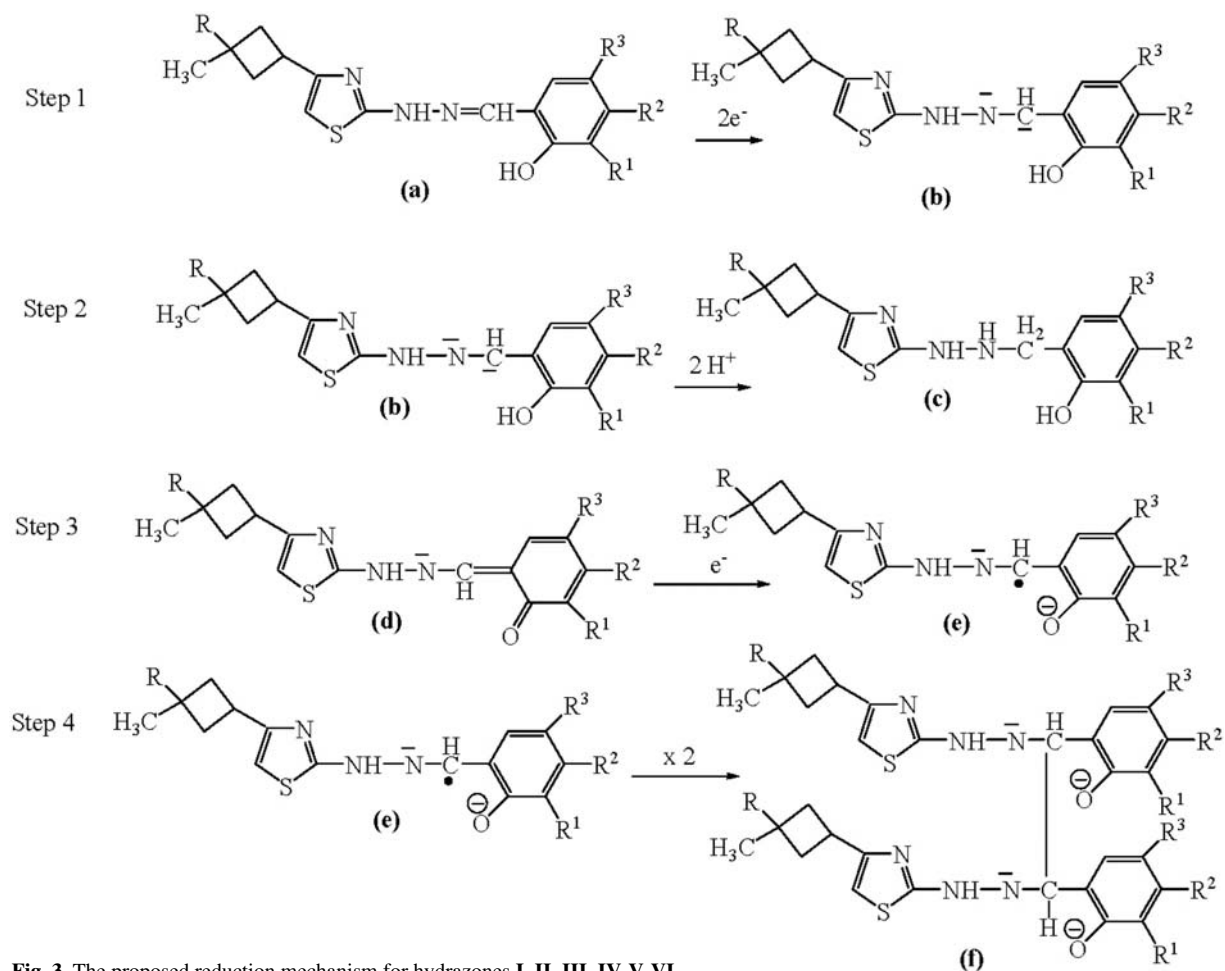


Fig. 3. The proposed reduction mechanism for hydrazones I, II, III, IV, V, VI.

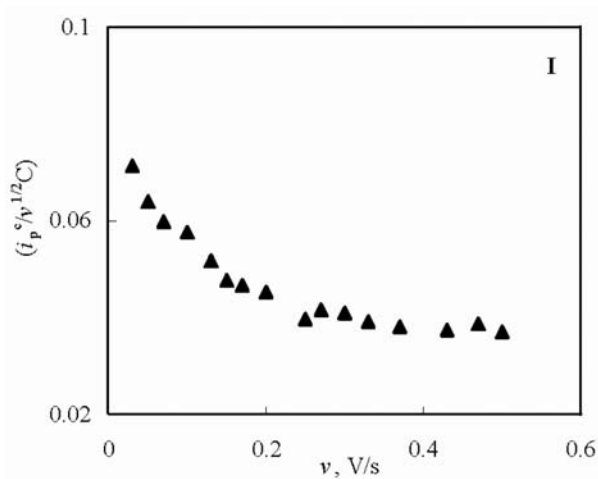


Fig. 4. ($i_p^c/v^{1/2}C$) versus scan rate v (V/s) plot of the first cathodic peak for 5.0×10^{-3} M I in DMF containing 0.1 M TBATFB.

One e^- transfer reaction in the second peak (Step 3) was most probably due to the reduction of product (d) formed as a result of the chemical reaction which took place after the first reduction. Fig. 7 shows the change of the current function of

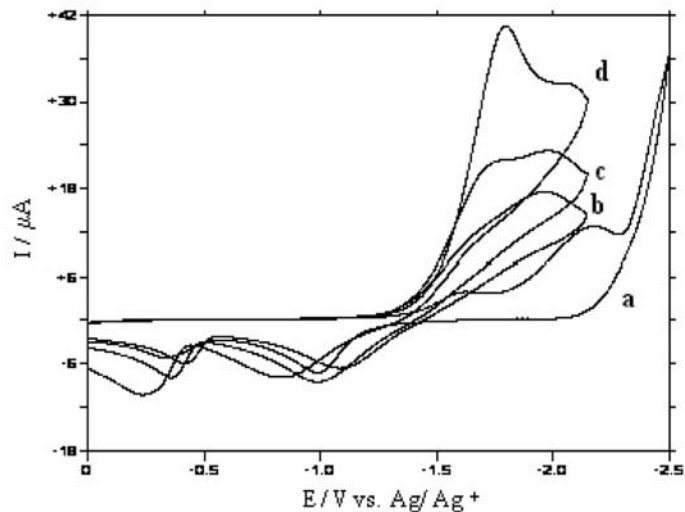


Fig. 5. Cyclic voltammograms of 5.0×10^{-3} M hydrazone I in DMF containing 0.1 M TBATFB at Pt electrode at $v = 0.1$ V/s: (a) hydrazone I alone; (b) after addition of mole acid/ mole hydrazone ratio of 1:4; (c) after addition of mole acid/ mole hydrazone ratio of 1:1; (d) after addition of mole acid/ mole hydrazone ratio of 2:1.

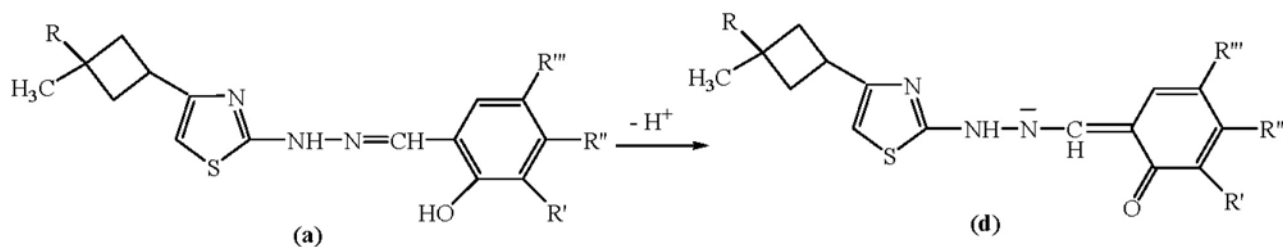


Fig. 6. The formation of conjugate base after a proton transfer step from non reduced molecules in solution.

peak (B) with the scan rate for hydrazone I. The decreasing trend in the resulting curve is the clear indication of the proceeding chemical reaction. The chemical step was thought to be the formation of a dimeric product (f) as a result of the combination of the radicalic species (e) after the electron transfer (Step 4). This is a mechanism suggested for similar molecules in literature.^{41,42,44,48,53} It is well-known that dimerization is an irreversible chemical reaction often involved in the electrodic processes with dianion derivatives.⁶⁶

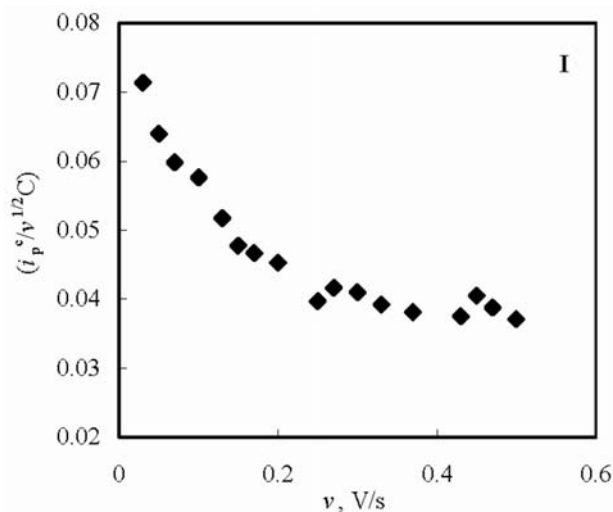


Fig. 7. ($i_p^c/v^{1/2}C$) versus scan rate v (V/s) plot of the second cathodic peak for 5.0×10^{-3} M I in DMF containing 0.1 M TBATFB.

4. Conclusions

This work has demonstrated that investigated hydrazones have two reduction and two oxidation peaks at platinum electrode in DMF. Based on the results obtained, the proposal of an electrode reaction mechanism pathway for these hydrazones can conveniently be claimed as ECEC mechanism. The electrochemical reduction occurs through acceptance of three electrons by successive two and one-electron irreversible peaks followed by chemical reactions. $E_p^c - E_{p/2}^c$ values were found to be 45–120 mV for each peak which is in good agreement with those given in literature for EC systems.⁶⁶

In order to test the validity of the proposed mechanism controlled-potential preparative electrolysis was carried out at the potential of the second peak for hydrazone

I and the reduction products were isolated. At the end of the electrolysis, the catholyte was poured into 200 mL of water and the reduction products were extracted with toluene. The toluene phase was dried over $MgSO_4$ and concentrated by rotary evaporation of the solvent. The reduction products were purified by column chromatography on silica gel using toluene/petroleum ether/ethanol/triethylamine (1 : 0.5 : 0.05 : 0.05) mixture. The isolated products were characterized with IR spectroscopy. The resulting spectrum showed that some of the characteristic bands of the parent hydrazone were disappeared (for instance C=N stretching band at 1625 cm^{-1}). This was taken as a further evidence for the proposed mechanism.

The electrochemical characteristics of these compounds investigated may be of use in future research on their action mechanism as well as pharmacokinetic and pharmacodynamic purposes in biological media, if they find use as drugs.

5. Acknowledgements

We gratefully acknowledge the financial support of Ankara University Research Fund (Project No: 2005-07-05-094).

6. References

1. M. Vinícius Nora de Souza, *J. Sulfur Chem.* **2005**, 26(4–5), 429–49.
2. L. Y. Wang, C. X. Zhang, Z. Q. Liu, D. Z. Lio, Z. H. Jang, S. P. Yan, *Inorg. Chem. Comm.* **2003**, 6, 1255–58.
3. A. H. Al-Dujaili, A. T. Atto, A.M. Al-Kurde, *Eur. Polym. J.* **2001**, 37, 927–32.
4. Y. Li, Y. Xu, X. Qian, B. Qu, *Tetrahedron Lett.* **2004**, 45, 1247–51.
5. V. C. Rucker, S. Foister, C. Melander, P. B. Dervan, *J. Am. Chem. Soc.* **2003**, 125(5), 1195–1202.
6. Q. Wang, H. Li, Y. Li, R. Huang, *J. Agric. Food Chem.* **2004**, 52, 1918–22.
7. K. Yanagimoto, K. G. Lee, H. Ochi, T. Shibamoto, *J. Agric. Food Chem.* **2002**, 50(19), 5480–84.
8. M. E. Abdel-Fattah, E. E. Salem, M. A. Mahmoud, *Ind. J. Heterocycl. Chem.* **2000**, 10(2) 121–28.
9. I. Yıldı, H. Perçiner, M. F. Sahin, U. Abbasoglu, *Arch.*

- Pharm.* **1995**, 328, 547–49.
10. Z. Cesur, S. Büyüktimkin, N. Büyüktimkin, *Arch. Pharm.* **1990**, 323(3) 141–44.
 11. E. Roger, C. J. Pierre, V. Pualette, G. Gerard, J. P. Chepat, G. Robert, *Eur. J. Med. Chem.* **1977**, 12(6), 501–9.
 12. G. Gerard, E. Roger, C. J. Pierre, J. C. Rossi, J. P. Girard, *Eur. J. Med. Chem.* **1979**, 14(6), 493–97.
 13. E. V. Dehmlow, S. S. Schmidt, *Liebigs Ann. Chem.* **1990**, 5, 411–14.
 14. R. B. Singh, *Talanta* **1982**, 29, 77–84.
 15. S. Zbaida, *Drug Metab. Rev.* **1995**, 27(3), 497–516.
 16. M. S. Baymak, H. Celik, H. Lund, P. Zuman, *Electrochem. Soc.* **2003**, 12, 94–96.
 17. M. Aleksic, V. Kapetanovic, P. Zuman, *Collect. Czech. Chem. Commun.* **2004**, 69, 1429–42.
 18. H. Lund, *Acta Chem. Scand.* **1959**, 13(2), 249–67.
 19. H. Lund, *Electrochim. Acta* **1983**, 28(3), 395–96.
 20. R. N. Goyal, R. Bhushan, A. Agarwal, *J. Electroanal. Chem.* **1984**, 171, 281–91.
 21. M. S. Baymak, P. Zuman, *Tetrahedron Lett.* **2006**, 47, 7991–93.
 22. V. Kameswara-Rao, C. S. Venkatachalam, C. Kalidas, *Ind. J. Chem.* **1987**, 26A, 202–4.
 23. H. M. Fahmy, *Annali di Chimica* **1985**, 75, 457–73.
 24. W. U. Malik, R. N. Goyal, M. Rajeshwari, *Bull. Soc. Chim. Fr.* **1987**, 1, 78–82.
 25. W. U. Malik, R. N. Goyal, R. Jain, *Talanta* **1977**, 24, 586–88.
 26. W. U. Malik, R. N. Goyal, P. N. Dua, *Electrochim. Acta* **1982**, 27(1), 25–31.
 27. H. M. Fahmy, G. E. H. Elgemeie, M. A. Aboutabl, B. N. Barsoum, Z. M. El-Massry, *Ind. J. Chem.* **1994**, 33B, 859–64.
 28. M. I. Ismail, *J. Chem. Technol. Biotechnol.* **1991**, 51, 155–69.
 29. C. J. Patil, A. S. Madhav, G. Ramachandriah, D. N. Vyas., *Ind. J. Chem.* **1994**, 33A, 1037–41.
 30. I. S. El-Hallag, G. B. El-Hefnawy, Y. I. Moharram, E. M. Ghoneim, *Can. J. Chem.* **2000**, 78, 1170–77.
 31. M. S. Baymak, H. Celik, H. Lund, P. Zuman, *J. Electroanal. Chem.* **2006**, 589, 7–14.
 32. M. S. Baymak, H. Celik, H. Lund, P. Zuman, *J. Electroanal. Chem.* **2005**, 581, 284–93.
 33. S. Çakır, E. Biçer, M. Odabaşoğlu, Ç. Albayrak, *J. Braz. Chem. Soc.* **2005**, 16(4), 711–17.
 34. M. S. Baymak, H. Celik, J. Ludvik, H. Lund, P. Zuman, *Tetrahedron Lett.* **2004**, 45, 5113–15.
 35. V. Kameswara Rao, C. S. Venkatachalam, C. Kalidas, *Bull. Chem. Soc. Jpn.* **1988**, 61, 612–14.
 36. H. Çelik, J. Ludvik, P. Zuman, *Electrochim. Acta* **2006**, 51, 5845–52.
 37. M. A. Gomez Nieto, M. D. Luque de Castro, M. Valcarcel, *Electrochim. Acta* **1983**, 28(12), 1725–32.
 38. H. Celik, G. Ekmekci, J. Ludvik, J. Picha, P. Zuman, *J. Phys. Chem. B.* **2006**, 110, 6785–96.
 39. J. M. Sevilla, C. Gregoria, T. Pineda, M. Blázquez, *J. Electroanal. Chem.* **1995**, 381, 179–83.
 40. R. N. Goyal, *J. Sci. Ind. Res.* **1992**, 51, 948–63.
 41. G. M. Abou-Elenien, N. A. Ismail, T. S. Hafez, *Bull. Chem. Soc. Jpn.* **1991**, 64, 651–54.
 42. A. A. Isse, A. Gennaro, E. Vianello, *Electrochim. Acta* **1997**, 42(13–14), 2065–71.
 43. J. M. Savéant, E. Vianello, *Electrochim. Acta* **1967**, 12, 1545–61.
 44. A. A. Isse, A. M. Abdurahman, E. Vianello, *J. Electroanal. Chem.* **1997**, 431, 249–55.
 45. A. J. Fry, R. G. Reed, *J. Am. Chem. Soc.* **1969**, 91(23), 6448–51.
 46. C. P. Andreux, L. Nadjo, J. M. Savéant, *Electroanal. Chem. Interfacial Electrochem.* **1970**, 26, 147–86.
 47. A. A. Isse, M. G. Ferlin, A. Gennaro, *J. Electroanal. Chem.* **2003**, 541, 93–101.
 48. M. Uçar, K. Polat, M. L. Aksu, H. Ünver, *Can. J. Chem.* **2004**, 82, 1–7.
 49. M. Uçar, K. Polat, M. L. Aksu, H. Ünver, *Anal. Sci.* **2004**, 20, 1179–83.
 50. T. Saied, M. L. Benkhoud, K. Boujlel, *Synth. Commun.* **2002**, 32(2), 225–33.
 51. B. Soucaze-Guillous, H. Lund, *J. Electroanal. Chem.* **1997**, 423, 109–14.
 52. A. A. El Maghraby, G. M. Abou-Elenien, N. A. Abdel-Reheem, H. R. Abdel-Tawab, *J. Korean Chem. Soc.* **2006**, 50(4), 307–14.
 53. G. M. Abou-Elenien, N. A. Ismail, M. M. Hassanin, A. A. Fahmy, *Can. J. Chem.* **1992**, 70, 2704–8.
 54. F. M. Triebe, M. D. Hawley, *J. Electroanal. Chem.* **1981**, 125, 421–35.
 55. J. M. W. Scott, W. H. Jura, *Can. J. Chem.* **1967**, 45, 2375–84.
 56. L. Nadjo, J. M. Savéant, *Electroanal. Chem. Interfacial Electrochem.* **1973**, 48, 113–45.
 57. L. V. Kononenko, V. D. Bezuglyi, V. N. Dmitrieva, *Zh. Obshch. Khim.* **1968**, 38 (10), 2153–9.
 58. A. Çukurovalı, İ. Yılmaz, *Pol. J. Chem.* **2000**, 74(1), 147–51.
 59. A. Çukurovalı, İ. Yılmaz, *J. Coord. Chem.* **2001**, 53(4), 329–37.
 60. A. Çukurovalı, İ. Yılmaz, H. Özmen, *Transition Met. Chem.* **2001**, 26(6), 619–24.
 61. A. Çukurovalı, İ. Yılmaz, *Synt. React. Inorg. Met.-Org. Chem.* **2003**, 33(4), 657–68.
 62. İ. Yılmaz, A. Çukurovalı, *Transition Met. Chem.* **2003**, 28, 399–404.
 63. İ. Yılmaz, Synthesis of some Schiff bases and their metal complexes, determination of their protonation and stability constants by potentiometric titration method, Ph.D Thesis, **2002**, Firat University, 97 pages, Elazığ, Turkey.
 64. A. S. Baranski, W. R. Fawcett, C. M. Gilbert, *Anal. Chem.* **1985**, 57(1), 166–70.
 65. R. J. Klingler, J. K. Kochi, *J. Phys. Chem.* **1981**, 85(12), 1731–41.
 66. R. S. Nicholson, I. Shain, *Anal. Chem.* **1964**, 36(4), 706–24.
 67. A. J. Bard, L. R. Faulkner, *Electrochemical Methods: Fundamentals and Applications*. John Wiley and Sons. Inc., New York, **2001**, 226–243.
 68. E. Laviron, *J. Electroanal. Chem.* **1980**, 112, 1–9.

Povzetek

S ciklično voltometrijo, elektrolizo s kontroliranim potencialom in kronoamperometrijo smo raziskovali elektrokemijske lastnosti šestih različnih spojin (hidrazonov) v prisotnosti 0.1 M tetrabutilamonijevega tetrafluoroborata. V območju med -1.60 V in -2.20 V smo opazili dva katodna vrhova. Z uporabo ultramikro elektrode smo določili difuzijske koeficiente in število prenesenih elektronov. Z metodo Klingler-Kochi smo izračunali konstante hitrosti. Predvidevamo, da proces elektrokemijske redukcije preiskovanih hidrazonov sledi ECEC mehanizmu